

# Peptide-Based, Two-Fluorophore, Ratiometric Probe for Quantifying Mobile Zinc in Biological Solutions

Daniel Y. Zhang,<sup>†</sup> Maria Azrad,<sup>‡</sup> Wendy Demark-Wahnefried,<sup>‡,§</sup> Christopher J. Frederickson,<sup>||</sup> Stephen J. Lippard,<sup>\*,†</sup> and Robert J. Radford<sup>\*,†</sup>

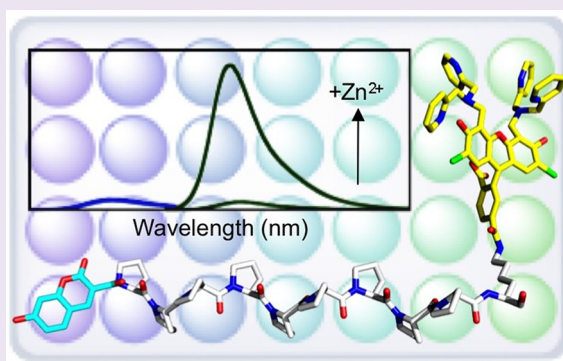
<sup>†</sup>Department of Chemistry, Massachusetts Institute of Technology, Cambridge, Massachusetts 02139, United States

<sup>‡</sup>Department of Nutrition Sciences and <sup>§</sup>Comprehensive Cancer Center, University of Alabama at Birmingham, Birmingham, Alabama 35294, United States

<sup>||</sup>Neurobiotex, 101 Christopher Columbus Boulevard, Galveston, Texas 77550, United States

## S Supporting Information

**ABSTRACT:** Small-molecule fluorescent sensors are versatile agents for detecting mobile zinc in biology. Capitalizing on the abundance of validated mobile zinc probes, we devised a strategy for repurposing existing intensity-based sensors for quantitative applications. Using solid-phase peptide synthesis, we conjugated a zinc-sensitive Zinpyr-1 derivative and a zinc-insensitive 7-hydroxycoumarin derivative onto opposite ends of a rigid P<sub>9</sub>K peptide scaffold to create HcZ9, a ratiometric fluorescent probe for mobile zinc. A plate reader-based assay using HcZ9 was developed, the accuracy of which is comparable to that of atomic absorption spectroscopy. We investigated zinc accumulation in prostatic cells and zinc levels in human seminal fluid. When normal and tumorigenic cells are bathed in zinc-enriched media, cellular mobile zinc is buffered and changes slightly, but total zinc levels increase significantly. Quantification of mobile and total zinc levels in human seminal plasma revealed that the two are positively correlated with a Pearson's coefficient of 0.73.



Zinc is an essential nutrient in biology.<sup>1</sup> Most biological zinc ions are tightly bound to proteins, functioning as catalytic or structural cofactors. In contrast, a small percentage of zinc is weakly bound to endogenous ligands and considered chelatable or mobile.<sup>2–4</sup> Mobile forms of zinc occur throughout the body and are capable of producing unique “zinc signals” critical to physiological functions of the endocrine/exocrine, immune, nervous, and reproductive systems.<sup>5–8</sup>

In the reproductive system, zinc is linked to male fertility,<sup>5,6</sup> oocyte maturation,<sup>9</sup> and cancer.<sup>10–12</sup> The healthy prostate contains large stores of zinc within the epithelium of the peripheral zone.<sup>6</sup> Zinc is released from secretory granules within epithelial cells into prostatic fluid, which comprises up to 30% of the volume of seminal fluid.<sup>6,13,14</sup> High zinc levels in seminal fluid enhance fertility by facilitating spermatozoa release from semenogelin proteins and promoting subsequent motility.<sup>5,15</sup> In cancerous prostate tissue, zinc levels are significantly reduced.<sup>6,10</sup> This reduction in zinc is not associated with adenoma or carcinoma but is found near sites of inflammation.<sup>8,10,16,17</sup> These observations suggest that zinc is intimately involved with oncogenesis, and if inflammation may be ruled out or treated, zinc could be used as a cancer-specific biomarker.<sup>10,17</sup> Understanding the physiology of prostatic zinc requires tools that can rapidly detect and quantify mobile zinc in complex environments such as cell lysate and biological fluids.

Fluorescent sensors are effective agents for investigating zinc biology.<sup>3,18,19</sup> Most zinc sensors consist of small-molecule fluorescent reporters derivatized with zinc-binding units. Extensive exploration in this field has yielded an array of small-molecule zinc probes with diverse photophysical and zinc-binding properties that have been validated in live cells, tissues, and animals.<sup>3,18,19</sup> Probes such as FluoZin-3, Newport Green, and Zinpyr-1 are intensity-based and increase in brightness ( $\epsilon\phi$ ) upon binding  $\text{Zn}^{2+}$  ions. Despite their utility, the inability to extract quantitative information using these probes is a major limitation.<sup>19</sup>

Ratiometric sensors offer a means to quantify mobile zinc concentration. The ratiometric response,  $R$ , is defined as the ratio of the emission intensity at two different wavelengths. In contrast to single-wavelength measurements from intensity-based sensors,  $R$  from dual-wavelength experiments is less sensitive to photobleaching and heterogeneous sample composition, which can globally alter the fluorescence intensity and lead to errors in the data or its misinterpretation. Although a number of ratiometric zinc sensors have been reported, we find relatively few instances of small-molecule sensors being

Received: August 2, 2014

Accepted: October 16, 2014

Published: November 10, 2014

used to quantify mobile zinc in biological solutions.<sup>19</sup> Complex syntheses, small dynamic ranges, and narrow gaps between the wavelengths used to determine *R* might be responsible for the limited application of these small-molecule ratiometric sensors in quantifying mobile zinc.

To overcome these challenges, we developed a synthetic strategy that uses solid-phase peptide synthesis to construct ratiometric zinc sensors. By coupling an intensity-based zinc probe to a zinc-insensitive fluorophore through a rigid polyproline spacer, we created a modular two-fluorophore assembly in which the zinc-sensitive and -insensitive units can be selected for specific applications. Similar small-molecule, two-fluorophore cassettes for ratiometric sensing have been developed for a variety of analytes, including zinc.<sup>20–22</sup> Most two-fluorophore systems that detect zinc, however, employ flexible linkers, which fail to separate the two fluorophores adequately and result in diminished photophysical properties.<sup>20–23</sup> Incorporation of a polyproline helix in our linker provides sufficient rigidity to our two-fluorophore system while, at the same time, exploiting the ease and modularity of solid-phase peptide synthesis.

As a proof-of-concept, we synthesized and characterized HcZ9, which joins a Zinpyr-1 (ZP1) derivative and a 7-hydroxycoumarin (Hc) derivative through a 10-residue peptide, P<sub>9</sub>K (Figure 1). A mobile zinc assay using HcZ9 was developed

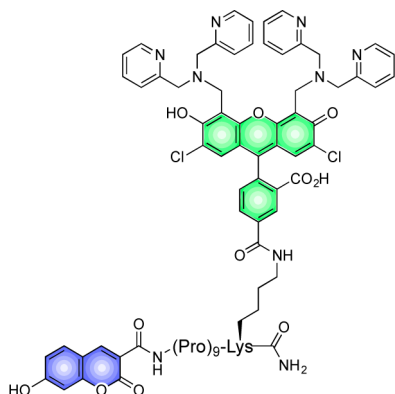


**Figure 1.** Representation of HcZ9, which features a 7-hydroxycoumarin derivative appended to the N-terminus of a peptide having the sequence P<sub>9</sub>K. A Zinpyr-1 derivative is coupled to the side chain of the C-terminal lysine residue.

that is compatible with standard fluorescence plate readers and quantifies zinc with accuracy comparable to that of zinc atomic absorption spectroscopy (AAS). Unlike zinc AAS, however, HcZ9 is selective for mobile zinc. In addition, the mobile zinc assay is much faster than current zinc AAS technology. HcZ9 was successfully applied to two case studies: (1) monitoring the change in mobile zinc levels when normal and malignant prostatic epithelial cells are bathed in zinc-enriched medium and (2) assessing the correlation between mobile zinc and total zinc in human seminal fluid. The results of these studies are presented here.

From the suite of existing intensity-based zinc sensors, green emitting 5-CO<sub>2</sub>H-ZP1 was selected as the zinc-sensitive fluorophore for its brightness, subnanomolar zinc-binding affinity, and compatibility with solid-phase peptide synthesis.<sup>24,25</sup> 5-CO<sub>2</sub>H-ZP1 is a representative member of the Zinpyr family of zinc sensors, which have zinc dissociation constants (*K*<sub>d-Zn</sub>) that span several orders of magnitude and have been extensively validated in living systems.<sup>3</sup> For the zinc-insensitive probe, we chose 7-hydroxycoumarin-3-carboxylic acid, a small, water-soluble fluorophore with a high fluorescence quantum yield, as well as absorption and emission bands that are distinct from those of ZP1. To separate the two fluorophores, we prepared a 10-residue (~31 Å) polyproline peptide with the sequence P<sub>9</sub>K. Polyproline peptides adopt rigid secondary structures that make them effective spacers for two-fluorophore systems.<sup>26</sup> The nine-residue polyproline motif was selected after an initial screen, which included three- and six-residue polyproline sequences.

The P<sub>9</sub>K peptide was synthesized using standard Fmoc-based chemistry. With orthogonal protecting groups, we sequentially added the Hc and ZP1 moiety to the N-terminus and C-terminal lysine side chain, respectively, to afford the resulting construct, Hc-P<sub>9</sub>K(ZP1)-CONH<sub>2</sub>, abbreviated as HcZ9 (Figure 1, Supplemental Figure S1). In addition, two singly labeled peptides, Hc-P<sub>9</sub>K and P<sub>9</sub>K(ZP1), were prepared to further probe the photophysical properties of HcZ9 (Supplemental Figure S2).

The zinc-binding and photophysical properties of HcZ9 were measured in buffer (50 mM PIPES and 100 mM KCl, pH 7) and are summarized in Supplemental Table S1. The absorption spectrum (Supplemental Figure S3) shows two principal maxima at 396 and 521 nm, which are assigned to the Hc and ZP1 moieties, respectively (Supplemental Figures S4 and

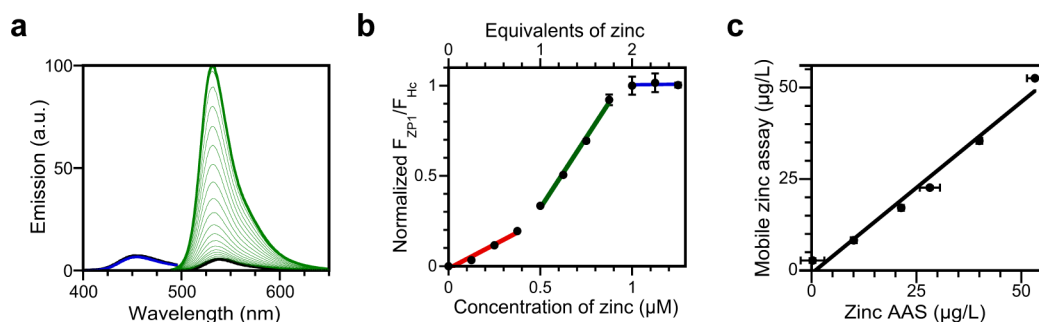


**Figure 2.** HcZ9 responds to zinc with a ratiometric change in fluorescence intensity. (a) Zinc-induced fluorescence enhancement of HcZ9. The zinc-insensitive Hc fluorophore is excited ( $\lambda_{\text{ex}}$ : 360 nm) and its fluorescence spectrum recorded (blue trace;  $\lambda_{\text{em}}$ : 400–495 nm). Separately, the ZP1 moiety is excited ( $\lambda_{\text{ex}}$ : 485 nm) and the fluorescence spectrum recorded (green trace;  $\lambda_{\text{em}}$ : 495–650 nm). (b) A representative calibration curve. The linear regions correspond to the first (red line) and second (green line) equivalents of Zn<sup>2+</sup> binding to ZP1, respectively, and finally stoichiometric saturation of the sensor (blue line). (c) Standard solutions of Zn(NO<sub>3</sub>)<sub>2</sub> were analyzed using AAS and the HcZ9. The linear fit shows a slope of 0.94  $\pm$  0.07 and a linear correlation coefficient of  $R^2 = 0.98$ . Data are means  $\pm$  SE.

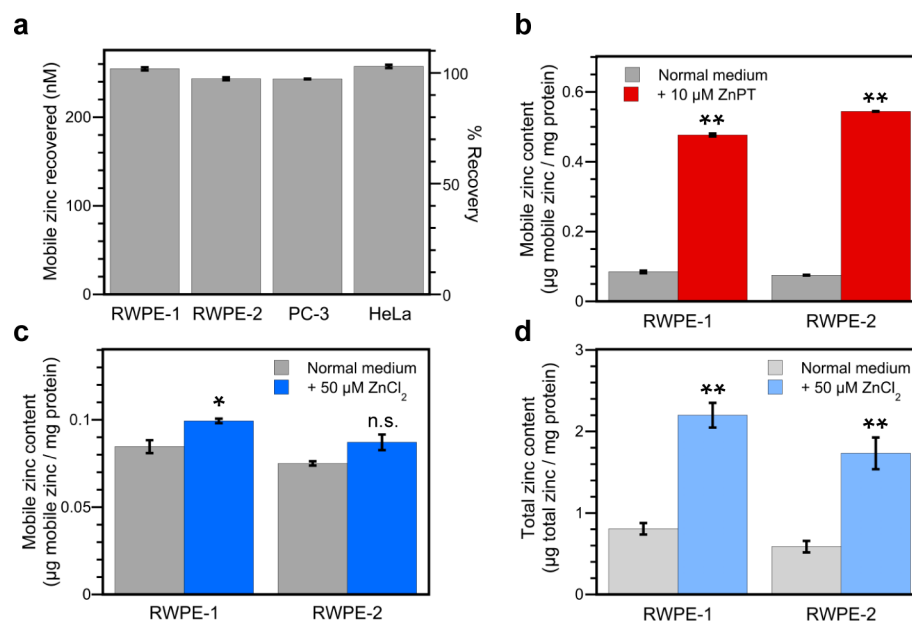


**Figure 3.** Mobile and total zinc measurements of cell lysates. (a) The mobile zinc concentration of cell lysate was measured before and after the addition of 250 nM (0.5 equiv) of ZnCl<sub>2</sub>. The measured increase in mobile zinc is shown in nM and compared to the expected increase (% recovery). (b) RWPE-1 and RWPE-2 cells were bathed for 30 min in either unmodified KSFM (gray bars) or KSFM supplemented with 10  $\mu$ M zinc pyrithione (ZnPT) (red bars). (c) Mobile and (d) total zinc concentrations in RWPE-1 and RWPE-2 cells were measured after cells were bathed for 24 h in either unmodified KSFM (gray bars) or in KSFM supplemented with 50  $\mu$ M ZnCl<sub>2</sub> (blue bars). The measured mobile zinc concentration is calculated relative to protein content. Data for total zinc in the RWPE cells were adapted from ref 28. Data are means  $\pm$  SE; n.s. is not significant; \* $p$  < 0.05; \*\* $p$  < 0.01.

S5). Circular dichroism spectroscopy suggests that HcZ9 adopts a polyproline type II helix conformation in aqueous buffer (Supplemental Figure S6).<sup>27</sup> Although HcZ9 can be used as a FRET-based sensor (Supplementary Figures S3–S5), independently exciting each fluorophore on HcZ9 increases the signal-to-background ratio, is compatible with a standard fluorescence plate reader, and reduces the effect of conformational changes due to interactions with biomolecules on the activity of the sensor. When HcZ9 operates as a dual-excitation, dual-emission sensor, the increase in the ratio of integrated fluorescence intensity,  $R$ , upon addition of excess ZnCl<sub>2</sub> is 5.3-fold. Here, we define the ratio,  $R$ , as  $R = F_{ZP1}/F_{Hc}$ , where  $F_{ZP1}$  is the integrated emission intensity for ZP1 ( $\lambda_{ex}$ : 485 nm;  $\lambda_{em}$ : 495–650 nm) and  $F_{Hc}$  is the integrated emission intensity for Hc ( $\lambda_{ex}$ : 360 nm;  $\lambda_{em}$ : 365–495 nm) (Figure 2a). HcZ9 was titrated with zinc in the presence of Ca-EDTA, a zinc buffering agent, to demonstrate mobile zinc detection and to determine an apparent zinc dissociation constant ( $K_{d,Zn}$ ) for HcZ9 of  $0.12 \pm 0.01$  nM (Supplemental Figure S8).<sup>3</sup> The ratiometric response is also selective for Zn<sup>2+</sup> over other biologically relevant divalent metal ions (Supplemental Figure S9).

Following validation of the ratiometric zinc response of HcZ9, we developed an assay for mobile zinc. Developing quantitative assays for mobile zinc in complex biological material will improve our understanding of zinc biology. Members of the Zinpyr family have been used to devise a fluorometric assay for mobile zinc,<sup>28–30</sup> but without ratiometric output these intensity-based sensors can be prone to artifacts. HcZ9, in contrast, offers the sensitivity and selectivity of the Zinpyr family but with the added advantage of ratiometric output.

For high-throughput analysis, the HcZ9-based mobile zinc assay was developed in a standard 96-well microplate format. A calibration curve was constructed by titrating a 1  $\mu$ M solution

of HcZ9 in buffer (50 mM PIPES and 100 mM KCl, pH 7) with an equal volume of standard zinc solutions.  $R$  is calculated from the fluorescence intensities, normalized, and plotted against total zinc concentration (Figure 2b). The resulting binding isotherm can be fit to three linear regions.<sup>31</sup> The first region corresponds to the formation of Zn:HcZ9 and leads to a response that is  $\sim 20\%$  of the maximal dynamic range. The second linear region correlates to the formation of Zn<sub>2</sub>:HcZ9 and yields a ratiometric response equal to  $\sim 80\%$  of maximal dynamic range. The third region occurs when the sensor is saturated with zinc and additional zinc ions will not further increase the fluorescence response.

Peptide-based compounds can be unstable in biological samples; however, HcZ9 was shown to exhibit sufficient stability under the assay conditions using fluorometric and HPLC methods (Supplemental Figure S10). To determine the accuracy of the mobile zinc assay, we prepared a series of standard zinc solutions and measured their zinc content using both Zn AAS and the HcZ9 probe (Figure 2c). Both techniques yielded similar results, indicating that the mobile zinc assay and zinc AAS have comparable accuracy (Figure 2c). The mobile zinc assay, however, offers several advantages over zinc AAS. HcZ9 selectively detects mobile zinc, whereas zinc AAS monitors total zinc. Moreover, our assay does not require expensive equipment, such as an AAS or related instrument, but instead employs more readily available fluorescence plate readers.

After confirmation that HcZ9 accurately measures mobile zinc concentrations under controlled conditions, we investigated its performance in cell lysates. For cell lines, we chose RWPE-1 and -2, PC-3, and HeLa. Spike and recovery experiments were performed to assess the accuracy of the method. In a typical experiment, the mobile zinc levels are measured before and after an addition of 250 nM (0.5 equiv)



ZnCl<sub>2</sub>. In all cell lines, the amount of spiked zinc measured was within 10% of the expected value (Figure 3a), suggesting that the activity of HcZ9 is not significantly altered by various biomolecules in these biological samples and validating the ability of HcZ9 to quantify mobile zinc in cell lysates (Supplemental Figure S11).

To study whether HcZ9 can measure changes in intracellular mobile zinc concentrations, cells were incubated for 30 min with 10  $\mu$ M zinc pyrithione (ZnPT), a membrane-permeable metal complex that rapidly delivers zinc into the cell.<sup>32</sup> After treatment with ZnPT, the resulting lysates showed a significant increase in mobile zinc levels (Figure 3, Supplemental Figure S10). Furthermore, the lysates also had a significant increase in total zinc (Supplemental Figure S12). Notably, the increase in total zinc was much greater than the increase in mobile zinc. In the RWPE cell lines, for example, treatment with ZnPT resulted in an increase of 3  $\mu$ g total Zn per mg protein, whereas the mobile zinc levels only increased by approximately 0.3  $\mu$ g of Zn per mg of protein. These results reveal that the cells can effectively buffer mobile zinc levels even when challenged with a large bolus of external zinc over a short period of time (Figure 3 and Supplemental Figure S12).

After validating the mobile zinc assay in cell lysates, we examined the relationship between total zinc and mobile zinc in prostatic cells. The RWPE lines represent a pair of genetically similar prostatic epithelial cells. RWPE-2 cells, however, express the v-Ki-ras oncogene and are tumorigenic.<sup>33</sup> RWPE-2 cells also have altered zinc trafficking pathways. Together, the RWPE lines have been used as model systems for investigating zinc biology in prostate cancer.<sup>34,35</sup> To monitor zinc accumulation, RWPE-1 and -2 cells were incubated for 24 h in either normal keratinocyte serum-free medium (KSFM) or KSFM supplemented with a total [ZnCl<sub>2</sub>] = 50  $\mu$ M. We specify total zinc because, owing to the buffer capacity of complete medium,<sup>28</sup> the available amount of mobile zinc is most likely less than 50  $\mu$ M. Mirroring the results with ZnPT addition treatment, both cell lines showed significant accumulation of total zinc but much smaller increases in mobile zinc (Figure 3c). We do note that by analyzing cell lysates, our reported values for mobile zinc content represent an average of all subcellular compartments; thus, any information regarding zinc trafficking pathways is lost. Given its facile nature and accuracy, however, our mobile zinc assay should prove useful in studying these levels in complex fluids or tissues at the cellular level.

To further demonstrate the utility of HcZ9, we measured total and mobile zinc in human seminal fluid. Evidence suggests that zinc in prostatic fluid correlates with prostate cancer, and it has been identified as a potential biomarker for the disease.<sup>10</sup> Moreover, mobile zinc levels have been directly linked to sperm motility and function.<sup>6,14</sup> There is a need for a rapid, accurate, and selective assay for mobile zinc in human seminal fluid.

We measured the mobile and total zinc content in seminal plasma from 107 prostate cancer patients that took part in a clinical study testing the effects of diet modification on prostate biology.<sup>36</sup> Prior work suggests that, after secretion, as much as 50% of zinc is redistributed and sequestered by medium and high molecular weight compounds from seminal vesicles.<sup>13</sup> Our data reveal a positive correlation (Pearson's  $r = 0.73$ ) between total and mobile zinc levels in seminal fluid (Figure 4). Interestingly, the correlation appears weaker at high zinc levels; further studies are needed to confirm and understand the apparent breakdown in the correlation at higher zinc levels.

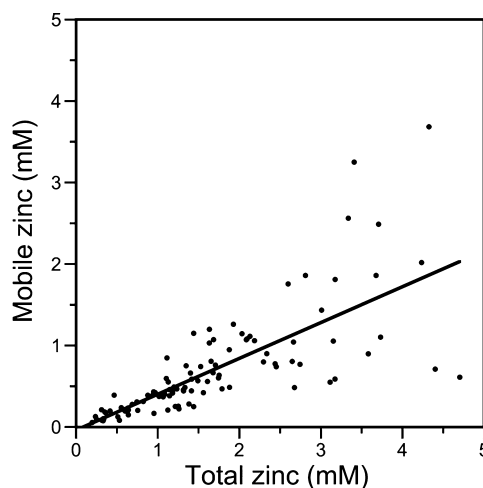


**Figure 4.** HcZ9 was used to measure mobile zinc content in 107 seminal fluid samples. The total zinc content for each sample was determined by zinc AAS. Pearson's  $r = 0.73$ ;  $n = 107$ .

In summary, we synthesized and characterized HcZ9, a peptide-based, ratiometric sensor for quantifying mobile zinc in biological solutions. Using HcZ9, a high-throughput mobile zinc assay was developed with comparable accuracy to zinc AAS. Our assay was applied to quantifying mobile zinc in epithelial prostatic cells and showed that both normal and tumorigenic cells maintain buffered mobile zinc levels even when challenged with exogenous zinc. In addition, HcZ9 was used to measure mobile zinc levels in human seminal plasma, revealing a positive correlation between the total and mobile zinc levels. The mobile zinc assay can be used with a variety of biological samples, such as homogenized tissue or organelle extracts, which would yield insight into changes in zinc homeostasis under different conditions. We envision that our synthetic strategy can generate ratiometric sensors for other of analytes, which would expand the chemical toolkit for determining concentrations of analytes in biological material.

## METHODS

See Supporting Information for a detailed description of the experimental methods.

## ASSOCIATED CONTENT

### Supporting Information

Details regarding the synthesis and characterization of HcZ9, as well as additional experiments, methods, and a detailed protocol for the mobile zinc assay are available free of charge via the Internet at <http://pubs.acs.org>.

## AUTHOR INFORMATION

### Corresponding Authors

\*(S.J.L.) E-mail: [lippard@mit.edu](mailto:lippard@mit.edu).

\*(R.J.R.) E-mail: [rradford@mit.edu](mailto:rradford@mit.edu).

### Notes

The authors declare no competing financial interest.

## ACKNOWLEDGMENTS

This work was supported by NIH grant GM065519 from the National Institute of General Medical Sciences to S.J.L. and NIH grant CA85740 from the National Cancer Institute to W.D.W. D.Y.Z. acknowledges MIT's UROP office and the Peter J. Eloranta Fellowship for support.

## REFERENCES

- (1) Maret, W. (2013) Zinc biochemistry: from a single zinc enzyme to a key element of life. *Adv. Nutr.* 4, 82–91.
- (2) Frederickson, C. J., Suh, S. W., Silva, D., Frederickson, C. J., and Thompson, R. B. (2000) Importance of zinc in the central nervous system: the zinc-containing neuron. *J. Nutr.* 130, 1471S–1483S.
- (3) Nolan, E. M., and Lippard, S. J. (2009) Small-molecule fluorescent sensors for investigating zinc metalloneurochemistry. *Acc. Chem. Res.* 42, 193–203.
- (4) Costello, L. C., Fenselau, C. C., and Franklin, R. B. (2011) Evidence for operation of the direct zinc ligand exchange mechanism for trafficking, transport, and reactivity of zinc in mammalian cells. *J. Inorg. Biochem.* 105, S89–S99.
- (5) Jonsson, M., Linse, S., Frohm, B., Lundwall, Å., and Malm, J. (2005) Semenogelins I and II bind zinc and regulate the activity of prostate-specific antigen. *Biochem. J.* 387, 447–453.
- (6) Kelleher, S. L., McCormick, N. H., Velasquez, V., and Lopez, V. (2011) Zinc in specialized secretory tissues: roles in the pancreas, prostate, and mammary gland. *Adv. Nutr.* 2, 101–111.
- (7) Radford, R. J., and Lippard, S. J. (2013) Chelators for investigating zinc metalloneurochemistry. *Curr. Opin. Chem. Biol.* 17, 129–136.
- (8) Haase, H., and Rink, L. (2014) Multiple impacts of zinc on immune function. *Metallomics* 6, 1175–1180.
- (9) Kim, A. M., Vogt, S., O'Halloran, T. V., and Woodruff, T. K. (2010) Zinc availability regulates exit from meiosis in maturing mammalian oocytes. *Nat. Chem. Biol.* 6, 674–681.
- (10) Costello, L. C., and Franklin, R. B. (2009) Prostatic fluid electrolyte composition for the screening of prostate cancer: a potential solution to a major problem. *Prostate Cancer Prostatic Dis.* 12, 17–24.
- (11) Franz, M.-C., Anderle, P., Bürzle, M., Suzuki, Y., Freeman, M. R., Hediger, M. A., and Kovacs, G. (2013) Zinc transporters in prostate cancer. *Mol. Aspects Med.* 34, 735–741.
- (12) Kolenko, V., Teper, E., Kutikov, A., and Uzzo, R. (2013) Zinc and zinc transporters in prostate carcinogenesis. *Nat. Rev. Urol.* 10, 219–226.
- (13) Owen, D. H., and Katz, D. F. (2005) A review of the physical and chemical properties of human semen and the formulation of a semen simulant. *J. Androl.* 26, 459–469.
- (14) de Lamirande, E. (2007) Semenogelin, the main protein of the human semen coagulum, regulates sperm function. *Semin. Thromb. Hemost.* 33, 60–68.
- (15) Malm, J., Jonsson, M., Frohm, B., and Linse, S. (2007) Structural properties of semenogelin I. *FEBS J.* 274, 4503–4510.
- (16) Kavanagh, J. P., Darby, C., and Costello, C. B. (1982) The response of seven prostatic fluid components to prostatic disease. *Int. J. Androl.* 5, 487–496.
- (17) Zaichick, V. Y., Sviridova, T. V., and Zaichick, S. V. (1996) Zinc concentration in human prostatic fluid: normal, chronic prostatitis, adenoma and cancer. *Int. Urol. Nephrol.* 28, 687–694.
- (18) Pluth, M. D., Tomat, E., and Lippard, S. J. (2011) Biochemistry of mobile zinc and nitric oxide revealed by fluorescent sensors. *Annu. Rev. Biochem.* 80, 333–355.
- (19) Carter, K. P., Young, A. M., and Palmer, A. E. (2014) Fluorescent sensors for measuring metal ions in living systems. *Chem. Rev.* 114, 4564–4601.
- (20) Woodroffe, C. C., and Lippard, S. J. (2003) A novel two-fluorophore approach to ratiometric sensing of  $Zn^{2+}$ . *J. Am. Chem. Soc.* 125, 11458–11459.
- (21) Woodroffe, C. C., Won, A. C., and Lippard, S. J. (2005) Esterase-activated two-fluorophore system for ratiometric sensing of biological zinc(II). *Inorg. Chem.* 44, 3112–3120.
- (22) Fan, J., Hu, M., Zhan, P., and Peng, X. (2013) Energy transfer cassettes based on organic fluorophores: construction and applications in ratiometric sensing. *Chem. Soc. Rev.* 42, 29–43.
- (23) Woo, H., You, Y., Kim, T., Jhon, G.-J., and Nam, W. (2012) Fluorescence ratiometric zinc sensors based on controlled energy transfer. *J. Mater. Chem.* 22, 17100–17112.
- (24) Radford, R. J., Chyan, W., and Lippard, S. J. (2013) Peptide-based targeting of fluorescent zinc sensors to the plasma membrane of live cells. *Chem. Sci.* 4, 3080–3084.
- (25) Radford, R. J., Chyan, W., and Lippard, S. J. (2014) Peptide targeting of fluorescein-based sensors to discrete intracellular locales. *Chem. Sci.* 5, 4512–4516.
- (26) Schuler, B., Lipman, E. A., Steinbach, P. J., Kumke, M., and Eaton, W. A. (2005) Polyproline and the "spectroscopic ruler" revisited with single-molecule fluorescence. *Proc. Natl. Acad. Sci. U.S.A.* 102, 2754–2759.
- (27) Rucker, A. L., and Creamer, T. P. (2002) Polyproline II helical structure in protein unfolded states: lysine peptides revisited. *Protein Sci.* 11, 980–985.
- (28) Bozym, R. A., Chimienti, F., Giblin, L. J., Gross, G. W., Korichneva, I., Li, Y., Libert, S., Maret, W., Parviz, M., Frederickson, C. J., and Thompson, R. B. (2010) Free zinc ions outside a narrow concentration range are toxic to a variety of cells in vitro. *Exp. Biol. Med.* 235, 741–750.
- (29) Frederickson, C. Meter for rapid analysis of unbound zinc in liquids. US Patent App. 11/221,167, 2005.
- (30) Zhang, X. A., Hayes, D., Smith, S. J., Friedle, S., and Lippard, S. J. (2008) New strategy for quantifying biological zinc by a modified zinpyr fluorescence sensor. *J. Am. Chem. Soc.* 130, 15788–15789.
- (31) Wong, B. A., Friedle, S., and Lippard, S. J. (2009) Solution and fluorescence properties of symmetric dipicolylamine-containing dichlorofluorescein-based  $Zn^{2+}$  sensors. *J. Am. Chem. Soc.* 131, 7142–7152.
- (32) Huang, Z., and Lippard, S. J. (2012) Illuminating mobile zinc with fluorescence from cuvettes to live cells and tissues. *Methods Enzymol.* 505, 445–468.
- (33) Bello, D., Webber, M. M., Kleinman, H. K., Wartinger, D. D., and Rhim, J. S. (1997) Androgen responsive adult human prostatic epithelial cell lines immortalized by human papillomavirus 18. *Carcinogenesis* 18, 1215–1223.
- (34) Chyan, W., Zhang, D. Y., Lippard, S. J., and Radford, R. J. (2014) Reaction-based fluorescent sensor for investigating mobile  $Zn^{2+}$  in mitochondria of healthy versus cancerous prostate cells. *Proc. Natl. Acad. Sci. U.S.A.* 111, 143–148.
- (35) Huang, L., Kirschke, C. P., and Zhang, Y. (2006) Decreased intracellular zinc in human tumorigenic prostate epithelial cells: a possible role in prostate cancer progression. *Cancer Cell Int.* 6, 10.
- (36) Demark-Wahnefried, W., Polascik, T. J., George, S. L., Switzer, B. R., Madden, J. F., Ruffin, M. T., Snyder, D. C., Owzar, K., Hars, V., Albala, D. M., Walther, P. J., Robertson, C. N., Moul, J. W., Dunn, B. K., Brenner, D., Minasian, L., Stella, P., and Vollmer, R. T. (2008) Flaxseed supplementation (not dietary fat restriction) reduces prostate cancer proliferation rates in men presurgery. *Cancer Epidemiol. Biomarkers Prev.* 17, 3577–3587.